Stability of a Penning trap with a quadrupole rotating electric field

T. Hasegawa,[1,2] M. J. Jensen,[1,*] and J. J. Bollinger[1,†]

[1]*Time and Frequency Division, National Institute of Standards and Technology, Boulder, Colorado 80305, USA*
[2]*Department of Material Science, University of Hyogo, Hyogo 678-1297 Japan*

We present theoretical and experimental studies of the center-of-mass (c.m.) stability of ions in a Penning trap with a quadrupole rotating electric field. The rotation frequency of an ion cloud in a Penning trap determines the cloud density and shape, and it can be precisely controlled by a rotating electric field. The quadrupole rotating-field scheme can control pure single-species plasmas in contrast to the dipole field, which is effective only for plasmas composed of two or more species of ions. However, the quadrupole field can modify the trap stability because of the spatial dependence of the electric field. In this study, we theoretically and experimentally determine the c.m. stability condition for ions in a Penning trap with a rotating quadrupole field. The experimental results agree well with the theoretical prediction. In the limit of zero magnetic field we obtain a type of rf trap which uses a rotating quadrupole field and in which the c.m. motion is analytically solvable.

I. INTRODUCTION

Plasmas consisting of particles with a single sign of charge (non-neutral plasmas), such as electrons, atomic ions, or positrons stored in a Penning trap or a rf trap [1–9] are interesting subjects of study in atomic physics and plasma physics—in particular, strongly coupled plasma physics [10]. Laser-cooled atomic-ion plasmas not only provide a particularly good example of a strongly coupled plasma, but are used in high-precision spectroscopy [11] and quantum-information processing [12] studies as well. In this article we study the stability of the center-of-mass (c.m.) motion in a Penning trap. Some of the results derived here for the Penning trap can also be applied to the rf trap by setting the magnetic field (i.e., the ion cyclotron frequency) to zero.

In a Penning trap, a static electric field generated by at least three trap electrodes and a static, uniform magnetic field B pointing in the z direction confine the charged particles [13]. We consider the case where the trap electrodes are large compared to the size of the trapped ion cloud. In this case, image charges on the trap electrodes can be neglected and the trap potential can be approximated by a static, quadrupole potential. In this limit the c.m. motion of the plasma separates from the internal degrees of freedom of the plasma. In general, the c.m. motion is a superposition of an axial oscillation (axial frequency $\omega_z/2\pi$), a circular cyclotron motion (modified cyclotron frequency $\Omega_m/2\pi$), and a circular magnetron motion (magnetron frequency $\omega_m/2\pi$). These frequencies are given by [13]

$$\omega_z = \beta \sqrt{\frac{eV_t}{m}}, \tag{1}$$

$$\Omega_m = \frac{1}{2}(\Omega + \sqrt{\Omega^2 - 2\omega_z^2}), \tag{2}$$

$$\omega_m = \frac{1}{2}(\Omega - \sqrt{\Omega^2 - 2\omega_z^2}). \tag{3}$$

Here, e and m are the charge and mass, respectively, of the trapped particles, V_t the dc voltage applied between the ring and the end-cap electrodes, β a geometric factor with dimensions of $(\text{length})^{-1}$ determined by the electrode configuration, and $\Omega = eB/m$ the cyclotron frequency.

Due to the $\mathbf{E} \times \mathbf{B}$ fields, a plasma in a Penning trap undergoes a rotation about the z axis of the trap. This rotation is uniform (does not depend on the radial position of an ion) in thermal equilibrium. The rotation frequency ω_r determines the plasma shape and density [10] and for stable confinement must satisfy $\omega_m < \omega_r < \Omega_m$. The plasma rotation ω_r can be precisely controlled by the rotating-field technique or, as it is sometimes called, the rotating-wall technique [14]. In this technique, an additional electric field that rotates about the z axis with angular frequency ω_w is applied. The rotating electric field applies a force that tends to make the plasma rotation synchronize with the field rotation ($\omega_r = \omega_w$). For synchronization, ω_r should be close to ω_w, otherwise the plasma slips relative to the rotating electric field and the rotating electric field provides very little control. The spatial dependence of the rotating field in a plane perpendicular to the magnetic field is typically constant (dipole field) or linear (quadrupole field), as shown in Fig. 1. The dipole rotating field can control the plasma rotation only if the c.m. is separated from the center of charge and is effective only for plasmas composed of two or more species of ions [14]. The quadrupole rotating field (QRF), on the other hand, can control pure single-species plasmas by distorting the plasma shape. However, the QRF can modify the resonant frequencies (Ω_m and ω_m) and even the trap stability, because an ac

*Also at Center for Integrated Plasma Studies (CIPS), University of Colorado, Boulder, CO 80309, USA.
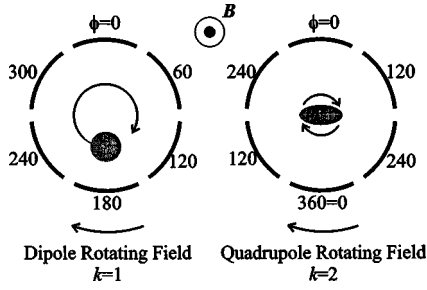†Electronic address: john.bollinger@boulder.nist.gov

FIG. 1. Dipole (left) and quadrupole (right) rotating-electric-field schemes for controlling the plasma rotation frequency. ac voltages $V_w \sin[k\omega_w t - \phi]$ with different phases ϕ are applied to a set of azimuthally segmented electrodes. The work discussed in this article used six azimuthally segmented electrodes, and the figure shows the phase ϕ for each electrode in this case. For a pure single-species plasma, the dipole field ($k=1$) does not couple with the plasma rotation, but does drive a circular c.m. motion of the plasma. The quadrupole field ($k=2$), on the other hand, distorts the plasma shape and can couple with the plasma rotation.

electric field with a spatial gradient can parametrically excite a c.m. motion of the plasma [8,15].

Dubin and O'Neil considered the confinement of a plasma in a Penning trap with a QRF in Ref. [10]. They derived criteria for when the effective potential of a Penning trap with a QRF is a quadratic potential well (as opposed to a saddle potential). The effective potential of a Penning trap is the apparent potential in a frame rotating with the QRF. Dubin and O'Neil [10] showed that an effective quadratic well potential leads to a confined thermally equilibrated plasma state. They did not consider what happens when the effective trap potential switches from a well to a saddle. The consequences of this switch for the plasma dynamics and confinement are not immediately apparent. In zero magnetic field, for example, a rotating saddle potential does give rise to stable confinement [16].

In this manuscript we solve the dynamical equations for the c.m. motion of a single-species plasma in a Penning trap with a QRF. We then determine the condition for when this motion is stable. For $\Omega^2 > 2\omega_z^2$ (required for stable trapping in a Penning trap without a QRF), this stability condition is the same condition given by Eq. (3.73) of Ref. [10] for when the effective trap potential switches from a well to a saddle. We also experimentally measure the c.m. stability condition for a weak QRF in the limit $\Omega \gg \omega_w > \omega_m$ and observe good agreement with the theoretical analysis.

II. INSTABILITY DUE TO THE QUADRUPOLE ROTATING FIELD

The electric potential provided by a rotating field of kth order can be expressed as

$$e\Phi_k = \frac{1}{2}m\omega_z^2 \delta_k r^k \cos[k(\theta + \omega_w t)], \quad (4)$$

where r and θ are cylindrical coordinates and δ_k is the amplitude of the rotating field normalized by the trap potential. The order k determines the spatial dependence of the rotating field and is equal to the number of cycles of Φ_k in 2π rads of the azimuthal direction. The dipole field corresponds to $k=1$ and the QRF to $k=2$. Hereafter, we discuss the case of $k=2$ only, and $\delta_2 = \delta$ is defined as a dimensionless quantity $\delta \equiv f_w V_w / V_t$. Here, f_w is a dimensionless geometric factor determined by the electrode configuration, and V_w is the voltage applied to the electrodes that generate the rotating field.

The c.m. motion of a single-species ion plasma in a Penning trap with a quadratic trap potential and a QRF separates from the internal degrees of freedom of the plasma. The equations of motion for the c.m. are

$$\frac{d^2x}{dt^2} = \Omega \frac{dy}{dt} + \frac{\omega_z^2}{2}x - \omega_z^2 \delta(x \cos 2\omega_w t - y \sin 2\omega_w t), \quad (5)$$

$$\frac{d^2y}{dt^2} = -\Omega \frac{dx}{dt} + \frac{\omega_z^2}{2}y + \omega_z^2 \delta(x \sin 2\omega_w t + y \cos 2\omega_w t), \quad (6)$$

$$\frac{d^2z}{dt^2} = -\omega_z^2 z. \quad (7)$$

The z-direction stability is always satisfied regardless of the QRF, and therefore we consider only the radial stability (x and y).

We introduce coordinates ξ and ζ defined by

$$x = \xi \cos \omega_w t + \zeta \sin \omega_w t,$$

$$y = \zeta \cos \omega_w t - \xi \sin \omega_w t. \quad (8)$$

ξ and ζ are coordinates in a frame rotating with the QRF. In terms of ξ and ζ we can rewrite Eqs. (5) and (6) as

$$\frac{d^2\xi}{dt^2} - (\Omega - 2\omega_w)\frac{d\zeta}{dt} + \left\{\omega_w(\Omega - \omega_w) - \left(\frac{1}{2} - \delta\right)\omega_z^2\right\}\xi = 0 \quad (9)$$

and

$$\frac{d^2\zeta}{dt^2} + (\Omega - 2\omega_w)\frac{d\xi}{dt} + \left\{\omega_w(\Omega - \omega_w) - \left(\frac{1}{2} + \delta\right)\omega_z^2\right\}\zeta = 0. \quad (10)$$

Note that the coefficients of the derivatives in Eqs. (9) and (10) are constants. The transformation of Eq. (8) has removed the explicit time dependence of Eqs. (5) and (6) on $\cos(2\omega_w t)$ and $\sin(2\omega_w t)$. Equations (9) and (10) can be combined into a fourth-order differential equation

$$\frac{d^4\xi}{dt^4} + b\frac{d^2\xi}{dt^2} + c\xi = 0, \quad (11)$$

where

$$b = (\Omega - 2\omega_w)^2 + 2\omega_w(\Omega - \omega_w) - \omega_z^2, \qquad (12)$$

$$c = \left\{ \omega_w(\Omega - \omega_w) - \frac{\omega_z^2}{2} \right\}^2 - \omega_z^4 \delta^2. \qquad (13)$$

The solution of Eq. (11) for real-valued ξ can be written

$$\xi = \sum_{j=1}^{2} (C_j e^{i\lambda_j t} + D_j e^{-i\lambda_j t}), \qquad (14)$$

where the C_j's and D_j's are complex constants determined from initial conditions, and the λ_j's are given by

$$\lambda_1 = \frac{1}{2}\sqrt{\Omega^2 - 2\omega_z^2 + (\Omega - 2\omega_w)^2 + 2\sqrt{4\omega_z^4\delta^2 + (\Omega - 2\omega_w)^2(\Omega^2 - 2\omega_z^2)}},$$

$$\lambda_2 = -\frac{1}{2}\sqrt{\Omega^2 - 2\omega_z^2 + (\Omega - 2\omega_w)^2 - 2\sqrt{4\omega_z^4\delta^2 + (\Omega - 2\omega_w)^2(\Omega^2 - 2\omega_z^2)}}. \qquad (15)$$

We verify that we can choose C_j's and D_j's to make ξ in Eq. (14) real. There are three cases to consider. The first is if λ_j is real (insides of the inner and outer square roots are positive); then $C_j = D_j^*$ makes ξ real. The second is if λ_j is imaginary (insides of the inner and outer square roots are positive and negative, respectively); then C_j and D_j should be real. The third case is if λ_j is complex (inside of the inner square root is negative). In this case $\lambda_1 = -\lambda_2^*$ (or $\lambda_1 = \lambda_2^*$ depending on how the principal value of the square root of complex numbers is chosen), and $C_1 = C_2^*$ and $D_1 = D_2^*$ (or $C_1 = D_2^*$ and $D_1 = C_2^*$) make ξ real.

If we assume the λ_j's are real, then Eq. (14) can be written in terms of two characteristic frequencies (λ_1 and λ_2) and two corresponding amplitudes (A_1 and A_2) and phases (ϕ_1 and ϕ_2) as

$$\xi = A_1 \cos(\lambda_1 t + \phi_1) + A_2 \cos(\lambda_2 t + \phi_2). \qquad (16)$$

From Eqs. (9) and (10) we observe that ζ is not independent of ξ. By substituting Eq. (16) for ξ in Eqs. (9) and (10), we obtain the following solution for ζ:

$$\zeta = \sum_{j=1}^{2} \frac{-\lambda_j^2 + \omega_w(\Omega - \omega_w) - \left(\frac{1}{2} - \delta\right)\omega_z^2}{\lambda_j(\Omega - 2\omega_w)} A_j \sin(\lambda_j t + \phi_j). \qquad (17)$$

The amplitudes (A_1 and A_2) and phases (ϕ_1 and ϕ_2) are determined from the initial conditions ($\xi, \zeta, d\xi/dt$, and $d\zeta/dt$ at $t=0$).

The c.m. orbit diverges exponentially when either λ_j in Eq. (15) has an imaginary part. Therefore, only if

$$\Omega^2 - 2\omega_z^2 + (\Omega - 2\omega_w)^2 \pm 2\sqrt{4\omega_z^4\delta^2 + (\Omega - 2\omega_w)^2(\Omega^2 - 2\omega_z^2)}$$
$$> 0 \qquad (18)$$

is satisfied will the c.m. motion be stable. For $\Omega^2 > 2\omega_z^2$ (required for stable trapping in a Penning trap without a QRF) Eq. (18) is always satisfied when we take the plus sign. With the minus sign we obtain the stability condition for the c.m. of

$$|\Omega^2 - 2\omega_z^2 - (\Omega - 2\omega_w)^2| > 4\omega_z^2|\delta|. \qquad (19)$$

As discussed in the Introduction, the condition of Eq. (19) is identical to that of Eq. (3.73) in Ref. [10] for when the effective trap potential changes from a quadratic well to a saddle potential.

As a special case, suppose a weak QRF is applied ($\delta \to 0$). We expect that Ω_m and ω_m can be derived from λ_1 and λ_2. For small δ and assuming $\omega_w > \omega_m$ we obtain

$$\lambda_1 = -\omega_w + \Omega_m + \frac{\omega_z^4}{2(\Omega - 2\omega_w)(\Omega - 2\omega_m)(\Omega_m - \omega_w)}\delta^2$$
$$+ O(\delta^4)$$

$$\lambda_2 = -\omega_w + \omega_m + \frac{\omega_z^4}{2(\Omega - 2\omega_w)(\Omega - 2\omega_m)(\omega_w - \omega_m)}\delta^2$$
$$+ O(\delta^4). \qquad (20)$$

We see that λ_1 and λ_2 approach, respectively, the modified cyclotron frequency and magnetron frequency in a frame rotating with ω_w. Note that for this case where the rotating-wall frequency ω_w is in the same direction and greater than the magnetron frequency ($\omega_w > \omega_m$), the magnetron frequency increases in proportion to δ^2. We note that this shift is opposite to what happens in the combined Penning-rf trap, where the addition of an oscillating (but *not* rotating) quadrupole field to a Penning trap decreases the magnetron frequency [17]. Finally, for our experimental work where the ordering $\Omega \gg \omega_w > \omega_m$ is valid, Eq. (20) can be approximated by

$$\lambda_1 = -\omega_w + \Omega_m + \frac{\omega_z^4}{2\Omega^3}\delta^2,$$

$$\lambda_2 = -\omega_w + \omega_m + \frac{\omega_z^4}{2\Omega^2(\omega_w - \omega_m)}\delta^2. \qquad (21)$$
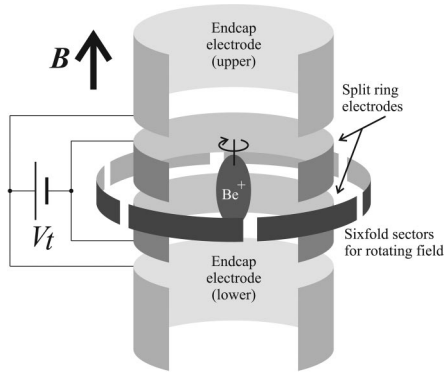
FIG. 2. Penning trap apparatus. Six azimuthally segmented electrodes outside the ring electrodes are used to provide the rotating electric field as shown in Fig. 1.

FIG. 3. Fluorescence intensity of ^{9}Be$^+$ ions as a function of the QRF frequency. Upper curve: the plasma was rotating faster than the QRF. Lower curve: the plasma was rotating synchronously with the QRF. In both cases, the QRF frequency was swept from higher to lower values.

From Eq. (19), the critical rotation frequency (ω_{cr}) of the QRF, which separates c.m. stability from instability, converges to ω_m when $\delta \to 0$. For $\Omega \gg \omega_w > \omega_m$, the critical frequency ω_{cr} obtained from Eq. (19) is given by

$$\omega_{cr} = \frac{\omega_z^2}{2\Omega} + \frac{\omega_z^2}{\Omega} f_w \frac{V_w}{V_t}. \tag{22}$$

Therefore the critical rotation frequency depends linearly on V_w. Because ω_z^2 is proportional to V_t, dependence on the trap voltage V_t occurs only in the first term of Eq. (22). Further, Eq. (22) is independent of mass m (note $\omega_z^2 \propto m^{-1}$ and $\Omega \propto m^{-1}$). This means that the critical frequency is not modified even in the case of plasmas composed of several species of ions.

III. EXPERIMENTS

We used the NIST Penning trap, discussed previously [14] to demonstrate the stability limits of a QRF. A sketch of the trap is shown in Fig. 2. The trap is housed in a vacuum chamber with a background pressure of 10^{-9} Pa. The 4.465 T magnetic field of the trap gives a ^{9}Be$^+$ cyclotron frequency $\Omega/2\pi$ of 7.608 MHz, and the axial frequency is described by Eq. (1), where $\beta\sqrt{e/m}$ is $2\pi \times 25.3$ kHz/V$^{1/2}$ for ^{9}Be. Trapped Be$^+$ ions are laser cooled by a 313 nm laser beam made by the second-harmonic generation of a 626 nm dye laser. The fluorescence of the trapped ions is detected by an imaging photomultiplier tube. The temperature of the laser-cooled ions is typically less than 10 mK, and the ion plasma forms a crystal. The plasma was not required to be a crystal for this study of the c.m. stability, but the high rate of laser scattering we obtained at low ion temperatures improved the signal-to-noise ratio.

The QRF is provided by sine waves applied with proper phases to the six azimuthal sectors located outside the ring electrode. The ring electrode is split into two sections along the z direction so that the QRF penetrates into the trap. The gap between the ring electrodes is also used for introducing a cooling laser beam directed perpendicular to the magnetic field and for the observation of the ion fluorescence. The geometric factor f_w was calculated to be 0.043 by solving
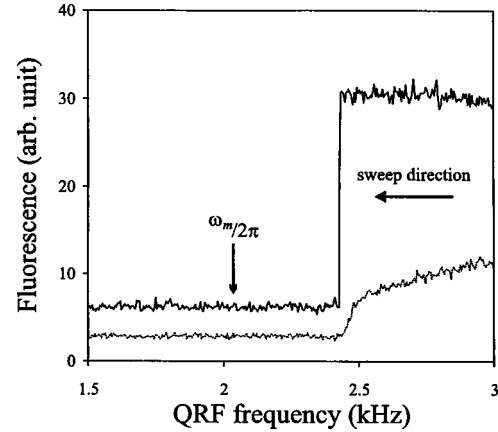
Laplace's equation with the boundary conditions of the trap electrodes, and experimentally determined to be 0.045 ± 0.007 by measuring the elliptical distortion of the plasma shape when the plasma was rotating synchronously with the QRF [14,18].

The critical QRF frequency ω_{cr} was measured by observing the fluorescence as ω_w was swept from higher to lower values. We expect that the ion plasma is lost and that the fluorescence becomes zero when ω_w coincides with ω_{cr}. Figure 3 shows examples of this observation. This measurement was carried out with $V_t = 48.5$ V and $V_w = 100$ V. One data set in Fig. 3 (upper curve) was taken with the plasma rotating faster than the QRF (namely, the ion plasma was slipping relative to the QRF), and the other data set (lower curve) was taken with the plasma rotating synchronously with the QRF. No difference was found in the critical frequency between the two data sets, that is, the rotation frequency of the ion plasma did not affect the c.m. stability, as expected theoretically. In both cases, the stability condition of the c.m. is so stringent that no ions survive for $\omega_w < \omega_{cr}$. The fluorescence of the lower curve becomes weak when the QRF frequency approaches the critical frequency. This is because the plasma density and rotation frequency decrease with ω_w for this case. The fluorescence of the upper curve, in contrast, remains constant until the QRF frequency reaches the critical frequency. This is because the plasma rotation and the density are independent of the QRF frequency when the ion plasma is slipping relative to the QRF. The critical rotation frequency is more precisely determined from the upper curve, and therefore we used the scheme in which the plasma is slipping for further measurements.

In Fig. 4, the critical frequency is plotted as a function of V_w with two values of V_t (48.5 and 28.5 V). The critical frequency depends linearly on V_w, as predicted by Eq. (22). Also, the two plots have the same slope with different $\omega_{cr}/2\pi$-axis intercepts. The $\omega_{cr}/2\pi$-axis intercept of each data set is the magnetron frequency $\omega_m/2\pi$. By comparing the slope of Fig. 4 and Eq. (22), f_w was determined to be 0.0480 ± 0.0005, which agrees well with the measured and
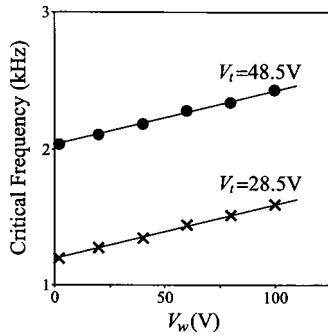
FIG. 4. Dependence of the critical frequency on V_w for two values of V_t. Circles and crosses are experimental results with fitted lines. The $\omega_{cr}/2\pi$-axis intercept of each data set corresponds to the magnetron frequency $\omega_m/2\pi$.

calculated values of f_w discussed earlier in this section. These results confirm the theoretical analysis in Sec. II.

IV. CONCLUSION AND DISCUSSION

We have shown theoretically and experimentally that the QRF modifies the stability of ions in Penning traps. From both the analysis of the c.m. equations of motion and measurements we find that for a given QRF amplitude, the c.m. stability depends not on the plasma rotation frequency but only on the frequency of the QRF. For a QRF frequency ω_w less than ω_{cr} given by Eq. (22), the ions are expelled from the trap. We obtained good agreement between theory and experiment. From this comparison we obtained a value for the geometric factor f_w that was more precise than that obtained by measuring the distortion of the plasma shape due to the QRF. The stability limit studied here implies that the QRF amplitude must be reduced for experimental work on oblate plasmas whose rotation frequency is only a little above the magnetron frequency.

The stability condition [Eq. (19)] we derived for $\Omega^2 > 2\omega_z^2$ is identical to the condition derived in Ref. [10] for when the effective trap potential changes from a quadratic well to a saddle potential. This result can be physically understood in the limit of large magnetic field and low rotation frequencies of the QRF. In this limit the effective magnetic field in a frame rotating with the QRF is large, and therefore the plasma c.m. motion in this rotating frame and in a direction perpendicular to the magnetic field is dominated by **E** $\times$ **B** drift [19]. When the effective potential in the rotating frame switches from a quadratic well to a quadratic saddle, the equipotential contours in a plane transverse to the magnetic field switch from closed ellipses to open hyperbolas. With **E** $\times$ **B** drift the plasma c.m. drifts along an equipotential surface. Therefore when this surface is an open hyperbola the plasma rapidly drifts out of the confinement region.

Finally we consider the special limiting case of zero magnetic field ($B \to 0$ and therefore $\Omega \to 0$). In this case, the stability condition for the c.m. motion becomes

$$1 < \frac{\sqrt{2}\omega_w}{\omega_z} < \delta < \frac{1}{2} + \frac{\omega_w^2}{\omega_z^2}. \tag{23}$$

The first inequality is due to the requirement that Eq. (18) is satisfied only if the sum of the terms to the left of the $\pm$ sign in Eq. (18) are positive. The next inequality in Eq. (23) is from the requirement of a positive argument of the square root in Eq. (18). Finally, the last inequality is from the requirement of Eq. (19). This ion-trapping scheme is recognized as a different type of radio-frequency (rf) trap. The characteristic frequencies of this rotating rf trap in a frame rotating with the QRF are given by

$$\omega_{rrf} = \sqrt{\omega_w^2 - \frac{\omega_z^2}{2} \pm \omega_z \sqrt{\delta^2 \omega_z^2 - 2\omega_w^2}}. \tag{24}$$

One advantage of the rotating rf trap is the simpler c.m. motion in this trap compared to the normal rf trap. The radial c.m. motion in a normal linear rf trap, which is described by a Mathieu equation, has an infinite number of Fourier components ($n\Omega_{rf} \pm \omega_{\text{secular}}$, where Ω_{rf} is the applied rf frequency, ω_{secular} is the secular frequency, and n is any integer) [13], whereas the radial c.m. motion in the rotating rf trap consists of four Fourier components [$-\omega_w \pm \omega_{rrf}$ in the laboratory frame where ω_{rrf} takes on two values from Eq. (24)]. This could mean, for example, that the optical spectral lines of energetic ions in the rotating rf trap are simpler than those in the normal rf trap because of fewer motional sidebands. As far as we know, the rotating rf trap is the only type of rf trap which is not expressed by a Mathieu-type solution.

The rotating rf trap is the electrical analog of the frictionless rotating-saddle trap, which was modeled and discussed in detail in Ref. [16]. The rotating-saddle trap consists of a ball confined in two dimensions by a rotating saddle-shaped surface and, of course, by gravity and the opposing vertical force of the surface in the third. This trap has been used to illustrate the principal of rf trapping for years. Reference [16] shows that for zero friction the motion of the ball perpendicular to the rotation axis is analytically solvable and consists of four Fourier components, in agreement with our conclusions above.

[1] *Non-Neutral Plasma Physics V*, edited by M. Schauer, T. Mitchell, and R. Nebel (AIP, New York, 2003).

[2] W. M. Itano, J. J. Bollinger, J. N. Tan, B. Jelenković, X.-P. Huang, and D. J. Wineland, Science **279**, 686 (1998).

[3] L. Hornekær and M. Drewsen, Phys. Rev. A **66**, 013412 (2002).

[4] E. M. Hollmann, F. Anderegg, and C. F. Driscoll, Phys. Rev. Lett. **82**, 4839 (1999).

[5] B. M. Jelenković, A. S. Newbury, J. J. Bollinger, W. M. Itano, and T. B. Mitchell, Phys. Rev. A **67**, 063406 (2003).

[6] R. G. Greaves and C. M. Surko, Phys. Rev. Lett. **85**, 1883 (2000).

[7] J. Estrada, T. Roach, J. N. Tan, P. Yesley, and G. Gabrielse, Phys. Rev. Lett. **84**, 859 (2000).

[8] P. Paasche, T. Valeuzuela, D. Biswas, C. Angelescu, and G. Werth, Eur. Phys. J. D **18**, 295 (2002).

[9] P. Paasche, C. Angelescu, S. Ananthamurthy, D. Biswas, T. Valenzuela, and G. Werth, Eur. Phys. J. D **22**, 183 (2003).

[10] D. H. E. Dubin and T. M. O'Neil, Rev. Mod. Phys. **71**, 87 (1999).

[11] J. J. Bollinger, D. J. Henizen, W. M. Itano, S. L. Gilbert, and D. J. Wineland, IEEE Trans. Instrum. Meas. **40**, 126 (1991).

[12] J. I. Cirac and P. Zoller, Phys. Rev. Lett. **74**, 4091 (1995).

[13] P. K. Ghosh, *Ion Traps* (Clarendon, Oxford, 1997).

[14] X.-P. Huang, J. J. Bollinger, T. B. Mitchell, W. M. Itano, and D. H. Dubin, Phys. Plasmas **5**, 1656 (1998).

[15] J. Tan and G. Gabrielse, Phys. Rev. A **48**, 3105 (1993).

[16] R. I. Thompson, T. J. Harmon, and M. G. Ball, Can. J. Phys. **80**, 1433 (2002).

[17] M. A. van Eijkelenborg, M. E. M. Storkey, D. M. Segal, and R. C. Thompson, Int. J. Mass. Spectrom. **188**, 155 (1999).

[18] The value of f_w is different from that in Ref. [14], because the electrodes used to provide the QRF in this experiment are different from those used in Ref. [14].

[19] D. H. E. Dubin and T. M. O'Neil, Phys. Rev. Lett. **60**, 511 (1988).